Model Evaluation of the Thermo-Hydrological-Mechanical Response in Argillaceous Sedimentary Rock Repository for Direct Disposal of Dual-Purpose Canisters

Fuel Cycle Research & Development

Prepared for

U.S. Department of Energy
Used Fuel Disposition Campaign

Liange Zheng[1]
Jonny Rutqvist[1]
Harris Greenberg[2]
Jens Birkholzer[1]

[1] *Lawrence Berkeley National Laboratory*
[2] *Lawrence Livermore National Laboratory*

June, 2014

FCRD-UFD-2014-000515
LBNL-6662E

Revision 2
12/20/2012

APPENDIX E

FCT DOCUMENT COVER SHEET [1]

Name/Title of Deliverable/Milestone/Revision No.	Model Evaluation of the Thermo-Hydrological Response in Argillaceous Sedimentary Rock Repository for Direct Disposal of Dual-Purpose Canisters
Work Package Title and Number	DR Disposal of Dual Purpose Canisters – LBNL FT-14LB081602
Work Package WBS Number	1.02.08.16
Responsible Work Package Manager	Jens Birkholzer (signature on file) (Name/Signature)

Date Submitted 06/30/2014

Quality Rigor Level for Deliverable/Milestone[2]	☐ QRL-3	☐ QRL-2	☐ QRL-1 ☐ Nuclear Data	☒ Lab/Participant QA Program (no additional FCT QA requirements)

This deliverable was prepared in accordance with Lawrence Berkeley National Laboratory
(Participant/National Laboratory Name)

QA program which meets the requirements of
☒ DOE Order 414.1 ☐ NQA-1-2000 ☐ Other

This Deliverable was subjected to:

☐ Technical Review ☐ Peer Review

Technical Review (TR) **Peer Review (PR)**

Review Documentation Provided **Review Documentation Provided**

☐ Signed TR Report or, ☐ Signed PR Report or,
☐ Signed TR Concurrence Sheet or, ☐ Signed PR Concurrence Sheet or,
☐ Signature of TR Reviewer(s) below ☐ Signature of PR Reviewer(s) below

Name and Signature of Reviewers

NOTE 1: *Appendix E should be filled out and submitted with the deliverable. Or, if the PICS:NE system permits, completely enter all applicable information in the PICS:NE Deliverable Form. The requirement is to ensure that all applicable information is entered either in the PICS:NE system or by using the FCT Document Cover Sheet.*

NOTE 2: *In some cases there may be a milestone where an item is being fabricated, maintenance is being performed on a facility, or a document is being issued through a formal document control process where it specifically calls out a formal review of the document. In these cases, documentation (e.g., inspection report, maintenance request, work planning package documentation or the documented review of the issued document through the document control process) of the completion of the activity along with the Document Cover Sheet is sufficient to demonstrate achieving the milestone. If QRL 1, 2, or 3 is not assigned, then the Lab/Participant QA Program (no additional FCT QA requirements box must be checked, and the work is understood to be performed, and any deliverable developed, in conformance with the respective National Laboratory/Participant, DOE- or NNSA-approved QA Program..*

This page is intentionally blank.

CONTENTS

FIGURES

TABLES

ACRONYMS

2-D	2-dimensional
3-D	3-dimensional
DPC	Dual-Purpose Canister
DSEF	Disposal Systems Evaluation Framework
DRZ	Disturbed Rock Zone
EBS	Engineered Barrier System
LLNL	Lawrence Livermore National Laboratory
NBS	Natural Barrier System
PWR	Pressurized Water Reactor
TH	Thermal and Hydrogeological
THM	Thermal, Hydrogeological and Mechanical
THMC	Thermal, Hydrogeological, Mechanical and Chemical
UFDC	Used Fuel Disposition Campaign

1. INTRODUCTION

The Used Fuel Disposition campaign (UFDC) is investigating geologic repositories for permanent disposal of high-level nuclear waste in different host rock environments (i.e. alluvium, clay, granites, salt), as well as different engineered barrier system (EBS) options with a variety of backfill materials. These natural and engineered materials present a range of thermal conductivities which act as a barrier to heat dissipation from the waste package to the host environment. Argillite is of particular interest as a host rock for waste disposal, due to its low permeability and low radionuclide diffusion coefficients, corresponding to a high retention capacity for radionuclides (Zheng et al., 2012). Furthermore, clay maintains self-sealing capabilities that retard radionuclide transport and inhibit microbial development, due to its swelling capacity when in contact with water (Hicks et al., 2009). These beneficial material properties make argillite or clay-based materials a desirable host rock and also backfill-material candidate. Recently, direct disposal of dual-purpose canisters (DPCs) in different media have been proposed (Hardin and Voegele, 2013). Preliminary analysis indicated that DPC direct disposal could be technically feasible, at least for certain disposal concepts (Hardin et al., 2013). Among several concepts for disposal of DPCs being proposed so far, one is the disposal of DPC in argillaceous sedimentary rock.

A DPC typically contains a high waste inventory of 32 PWR (Pressurized Water Reactor)fuel assemblies, which is much larger than the small canister (4 PWR) that has been widely studied in UFDC. It has therefore a higher heat-release rate. To avoid a large repository footprint or long-term surface storage, first, the temperature limit in an argillite repository must be raised above 100°C; second, ventilation of the drift may be required. However, several important issues must be addressed for better assessing the performance implications of the substantially higher temperature. For example, what is the hydrogeological alteration in the host rock during the ventilation period? Will the disturbed rock zone (DRZ) be enlarged? How will the host rock be chemically altered under oxidizing conditions caused by ventilation and the subsequent long-term exposure to high temperature? How will EBS bentonite respond geochemically to long-term heating (higher than 100°C) and hydration? How will the host rock and backfill material be mechanically altered? Moreover, strong thermal gradients will induce complex moisture-transport processes and bentonite-rock interactions affecting early disposal system behavior (pore pressure, vapor diffusion, bentonite resaturation, etc), for which the thermal (T), hydrological (H), mechanical (M) and chemical (C) processes are tightly coupled. How THMC processes will interact with each other is also an important issue.

To answer the questions above, extensive R&D is required, from detailed mechanistic THMC models of individual system components (waste package, EBS, NBS) to 2D (two-dimensional) and 3D (three-dimensional) models for understanding and predicting the EBS and host-rock perturbation, and eventually toward a performance assessment model for scenario analyses. Significant progress has been made in UFDC to understand the detailed THMC alteration of individual system components for disposal of small canisters in argillaceous host rock. Knowledge gained in these studies can also be applied to the disposal of DPC in argillite. However, in terms of using 2D and 3D models to predict the changes in backfill and argillaceous host rock, the disposal of DPC has some special features that differ from the disposal of small canisters, which make previous models developed for small canisters inapplicable. These features include an initial ventilation period, larger drift, asymmetric layout of waste package and backfill, and possibly a thicker concrete liner or steel liner to maintain stability. Therefore, disposal of DPCs in argillaceous host rock needs its own series of 2D and 3D models to evaluate the THMC processes in the backfill and argillaceous host rock for disposal of DPCs.

In this report, we document initial progress toward building 2D and 3D models to evaluate the THMC processes in the EBS and argillaceous host rock for disposal of DPCs. Specifically, the accomplishments to date in FY14 are:

1. Evaluating the desaturation of argillaceous host rock as a result of heating based on the temperature calculated by a Disposal Systems Evaluation Framework (DSEF). The purpose for doing this is twofold. First, DSEF is widely used for the thermal analysis for the disposal of DPCs (e.g., Hardin et al., 2013). It is based on analytical solutions of conduction-only heat transport, taking into account the heat contribution from adjacent drifts and waste packages. It is therefore easy to solve and powerful for analyzing design options, such as drift spacing and waste package spacing. However, because it is an analytical solution, several assumptions are necessary, thermal conductivity does not change with water saturation in the host rock, and the layout of the waste package and backfill is axi-symmetrical. Using a numerical simulator, TOUGH, to run a similar scenario, but allowing thermal conductivity to change with water saturation, provides a validation of the DSEF model. Second, we can evaluate the range of desaturation in the host rock and sensitive thermal and hydrogeological parameters that affect the desaturation.
2. Developing a 2-D THM model for more realistic layout geometry of waste package and backfill to examine the spatial variability of THM behavior in backfill and host rock.

After a brief introduction of the calculation tools, this report is structured based on these two accomplishments. In Section 3, we present the results of modeling the desaturation of host rock based on DSEF results, showing DSEF results first and TOUGH models second. In Section 4, we discuss the results of THM model for more realistic layout geometry of waste package and backfill. Finally, some preliminary observations and future research work are discussed.

2. SIMULATOR

The modeling work presented in this report is conducted with the DSEF (Greenberg et al., 2012) and TOUGH2 (Pruess et al., 1999). DSEF was developed at Lawrence Livermore National Laboratory (LLNL) to formalize and facilitate the development and documentation of repository conceptual design options for a range of waste forms, geologic environments, repository design concepts, and repository operating modes. Its core functionality is provided by a combination of a Microsoft Office Excel 2010 workbook, with macros and form controls that create a structured environment (to define the repository design concepts and input data), coupled with a Mathcad 15 analytical model that performs the transient heat transfer calculations (Greenberg et al., 2012). TOUGH2 is a numerical simulation program for nonisothermal multicomponent fluid and heat flow (Pruess et al., 1999). A broad range of subsurface thermo-physical–chemical processes are considered, and the program can be applied to one-, two- or three-dimensional porous and fractured media. The THM simulation was conducted with TOUGH-FLAC3D (Rutqvist et al., 2011) which sequentially couples the finite-difference geomechanical code FLAC3D (Itasca, 2009) with the finite-volume, multiphase fluid flow code, TOUGH2 (Pruess et al., 1999).

3. MODELING THE DESATURATION OF HOST ROCK BASED ON DSEF RESULTS

3.1 Thermal analysis with DSEF

In this report, two scenarios were analyzed with DSEF: a case in which the drift is ventilated for 40 years, referred to as “40-year ventilation,” and a case in which the drift is ventilated for 350 years, referred to as “350-year ventilation.” The 40-year ventilation scenario consists of a 32 PWR fuel assembly waste package with a drift spacing of 45 m between parallel tunnels, waste package spacing of 20 m along the tunnels, surface storage time of 50 years, and ventilation time of 40 years (after emplacement). The 350-year ventilation scenario is identical except that the ventilation period is 350 years and the waste package

spacing is 10 m. Both cases assume that the waste packages contain 40 GWd/MTHM (Gigawatt Day/ Metric Ton Heavy Metal) of UOX (Uranium Oxide) spent fuel. After ventilation, the drift is backfilled with bentonite.

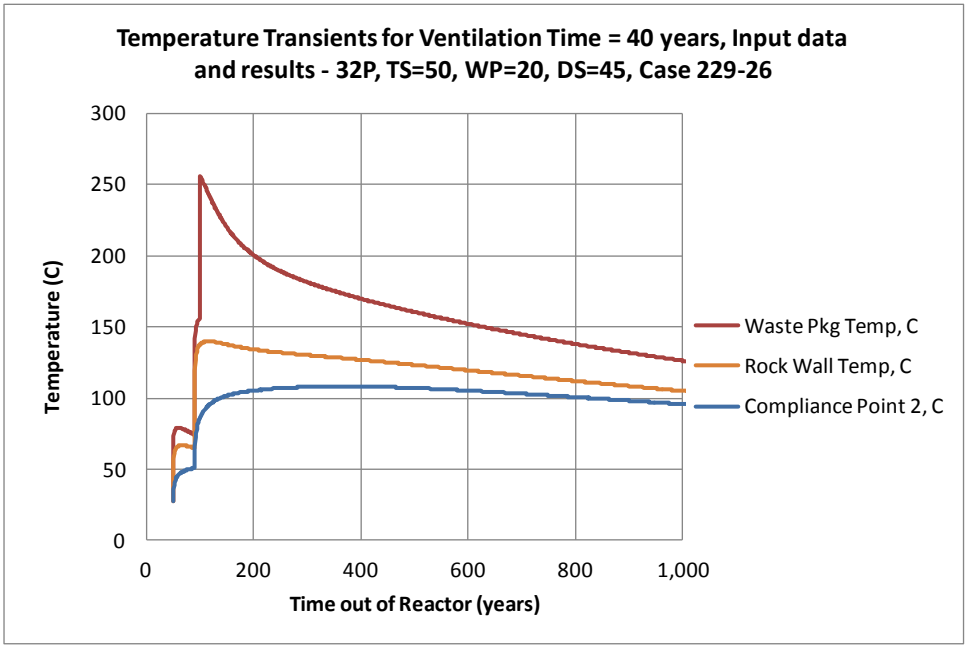

Figure 1. Temperature evolution at the surface of waste package, rock wall, and a compliance point with a radius of 5.25 m (3 m from the rock wall) for the 40-year ventilation scenario.

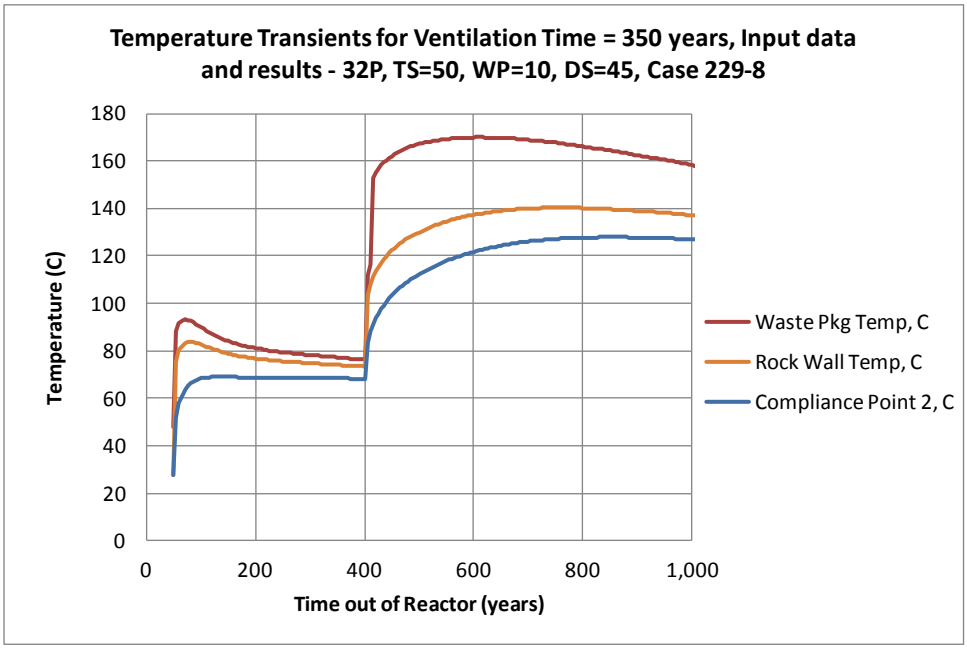

Figure 2. Temperature evolution at the surface of waste package, rock wall, and a compliance point with a radius of 5.25 m (3 m from the rock wall) for the 350-year ventilation scenario.

Figures 1 and 2 show the temperature profile at the rock wall for 40-year ventilation and 350-year ventilation scenarios, respectively. A maximum temperature of 140°C is reached in both cases, but with

longer ventilation, i.e. for the 350-year ventilation scenario, the waste package spacing is 10 m. On the other hand, for the 40-year ventilation scenario, a waste package spacing of 20 m is required.

3.2 TOUGH2 model for desaturation in the host rock

DSEF is a powerful tool for thermal analysis of disposal concepts, although some assumptions have to be made, as DSEF is essentially an analytical solution of the conductive heat transport. One of these assumptions is that the thermal conductivity in the host rock is constant. It is known that thermal conductivity of porous media is a function of the water saturation. During the ventilation period, it is expected that desaturation occurs in the host rock and therefore changes thermal conductivity. We therefore need to answer questions such as: What is the impact of the desaturation on the temperature profile in the host rock? How much inaccuracy is introduced by DSEF when assuming a constant thermal conductivity? To answer these questions, two steps are taken. First, DSEF results are reproduced with TOUGH2 models, which assume constant thermal conductivity; these TOUGH2 models are referred to as "base case" hereafter. Second, TOUGH2 simulations with saturation-dependent thermal conductivity were conducted. By comparing results from the first and second step, we can address the above questions.

3.2.1 TOUGH2 model setup

TOUGH2 models simulate a 2-D cross section (Figure 3) of the emplacement drift with surrounding argillite. The emplacement drift is located at 500 m depth (z-axis), with one-half of the horizontal drift spacing from center-to-center set at 22.5 m (x-axis). The EBS consists of the canister, initially surrounded by unsaturated air in contact with perforated steel liner and the rock wall, which is followed by backfilling of the tunnels. Symmetry assumptions allow replacing the set of parallel neighboring emplacement drifts with only one emplacement drift. Unit length is assumed in the y-direction, which is along the centerline of the emplacement drift. The tunnel radius is 2.26 m and is denoted in Figure 3 as (*). The space between the waste package and rock wall is open during the ventilation period, but backfilled with bentonite after ventilation ceases.

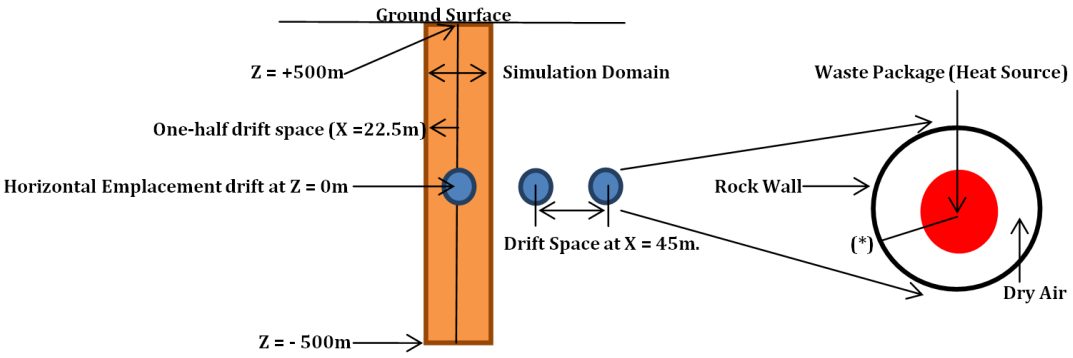

Figure 3. Repository layout for modeling drift at 500 m below ground surface

The pressure and temperature are fixed at the top and bottom of the simulation domain. During the ventilation period, time-dependent temperature boundary conditions are prescribed on the drift wall, while the relative humidity of the air in the drift tunnel is about 53%. The time-dependent temperature is based on the DSEF calculation. After ventilation ends, bentonite backfill with an initial gas saturation of 35% is emplaced. Table 3 lists the thermal and hydrodynamic parameters used in the model. Those parameters for the bentonite are largely taken from Sonnenthal (2008) except for thermal conductivity, which is the

same as that used in DSEF; those for the argillite are largely based on Opalinus Clay (Thury, 2002), except for thermal conductivity and permeability. Thermal conductivity is same as that in DSEF model. Regarding permeability, Soler (2001) reported that the Opalinus Clay has permeability ranging from 10^{-21} to 10^{-18} m^2, with lower values of 10^{-21} to 8×10^{-21} m^2 (Harrington and Horseman, 1999; De Windt and Palut, 1999) as evaluated from laboratory measurements, whereas higher value of 10^{-18} have been estimated from field tests (NAGRA, 1989). A permeability of $5.0\times10^{-19}m^2$ is used here.

Table 1. Thermal and hydrodynamic parameters for host rock and bentonite buffer

Parameter	Host rock	Bentonite backfill
Grain density [kg/m^3]	2700	2700
Porosity ϕ	0.15	0.39
Saturated permeability [m^2]	$5.0\cdot10^{-19}$	$5.0\cdot10^{-20}$
Relative permeability, k_{rl}	m = 0.6, S_{rl} = 0.01	$K_{rl} = S^3$
Van Genuchten α [1/Pa]	$6.8\cdot10^{-7}$	$3.3\cdot10^{-8}$
Van Genuchten m	0.6	0.3
Compressibility, β [1/Pa]	$3.2\cdot10^{-9}$	$5.0\cdot10^{-8}$
Thermal expansion coeff., [1/K]	0.0	$1.0\cdot10^{-4}$
Dry specific heat, [J/kg^{o}C]	800	1247
Thermal conductivity [W/m K]	1.48 (dry) / 1.75 (wet)*	0.6(dry)/1.2(wet)*
Tortuosity for vapor phase	$\phi^{1/3}S_g^{10/3}$	$\phi^{1/3}S_g^{10/3}$
Bulk modulus, (GPa)	4.17	0.02
Shear modulus, (GPa)	1.92	0.0067

*In the base model, thermal conductivity under "dry" conditions is 1.75 W/m K, to align with the DSEF model.

In the next subsection, we start with simulation cases in which we try to emulate the DSEF temperature calculation, the base case. The next step is then a series of cases in which we account for the saturation-dependent thermal conductivities of host rock.

3.2.2 RESULTS

3.2.2.1 Base Case

In TOUGH2, the thermal conductivity K_{th} is calculated as:

$$K_{th} = K_{wet} + S_l(K_{wet} - K_{dry}) \quad (1)$$

where K_{wet} is the thermal conductivity under fully liquid-saturated conditions, K_{dry} is the thermal conductivity under desaturated conditions, and S_l is the liquid saturation degree. In the base case, K_{wet} = K_{dry} = 1.75 W/m K, which means that thermal conductivity is unaffected by saturation changes.

40-Year Ventilation scenario

Figure 4 depicts the temperature profile simulated with TOUGH2 at the rock wall. Notice that the simulations start at 50 years, based on the assumption that waste packages are emplaced after 50 years of interim surface storage time. After emplacement, we see a quick temperature rise with a maximum around 65°C at rock wall. As ventilation continues (removing 75% of the decay heat generated by the waste packages), the heat output of the waste package slowly decreases. As ventilation stops 40 years later, there is another drastic increase in rock wall temperature, reaching about 140°C, indicating the necessity

of active ventilation to keep the repository temperature down. Temperature decreases gradually towards the far field in the rock. TOUGH2 and DSEF have practically the same temperature at the rock wall, because the TOUGH2 model uses the results from DSEF as boundary conditions. Deeper into the rock, a slight discrepancy is observed between results from the TOUGH2 model and DSEF, probably because DSEF is a 3-D model solved for the temperature adjacent to the centerline of a central waste package whereas TOUGH2 model is 2-D and represent an average condition along the waste package.

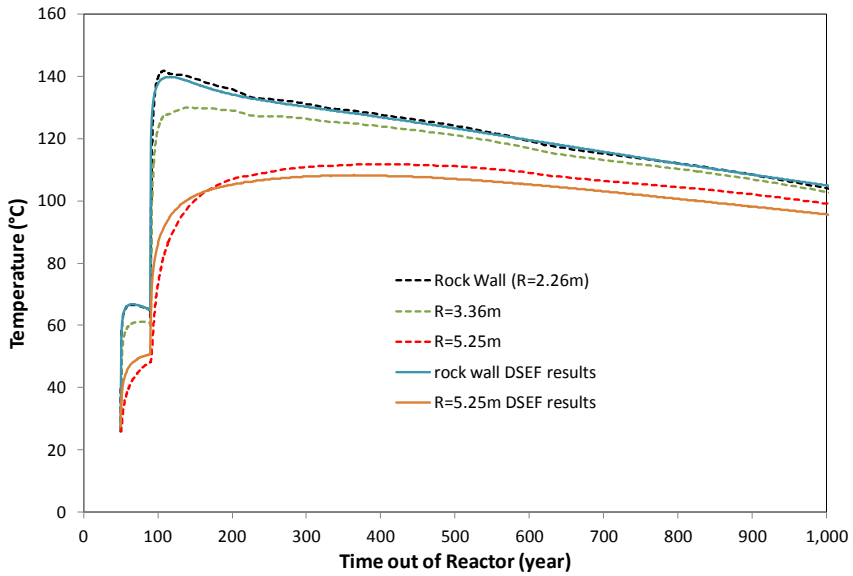

Figure 4. Temperature evolution at several compliance points for backfill and non-backfill operation modes for the 40-year ventilation scenario.

Gas saturation profiles for several compliance points are plotted in Figure 5. Ventilation causes desaturation in the host rock during the ventilation period, but this effect does not persist very far away from the tunnel. At the point immediately next to the tunnel wall, gas saturation increases to a maximum of ~0.48, but just 0.3 meters further inside, the host rock the gas saturation is only ~0.25. No desaturation effect can be seen at a radial distance of 5.25 meters and beyond. As ventilation ceases, there is no strong driving force for drying out the near-field host rock, and the system resaturates within about 10 years.

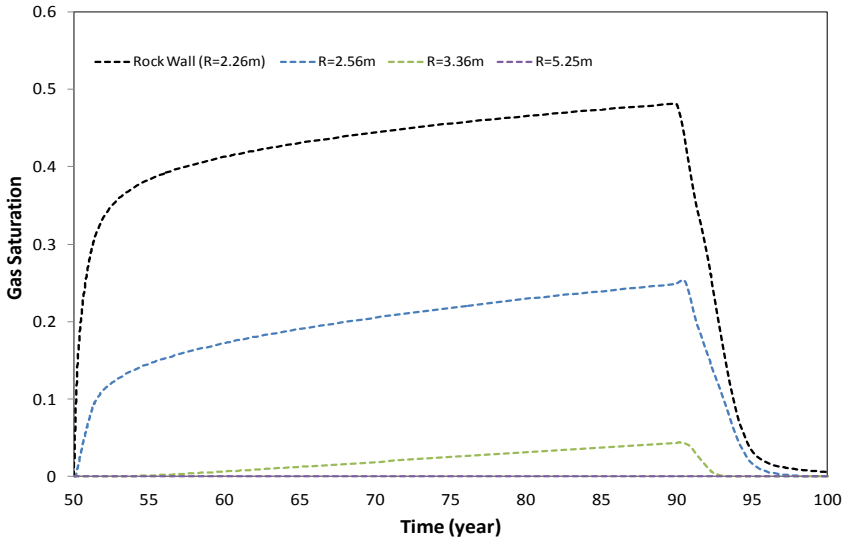

Figure 5. Gas saturation evolution at several compliance points for the 40-year ventilation scenario.

350-Year Ventilation scenario

Thermal transients at multiple compliance points are shown in Figure 6 for the 350-year ventilation scenario. Like the 40-year ventilation scenario, TOUGH2 model results are similar to that from DSEF. Ventilation keeps the temperature low, after which the host rock undergoes a sharp temperature increase.

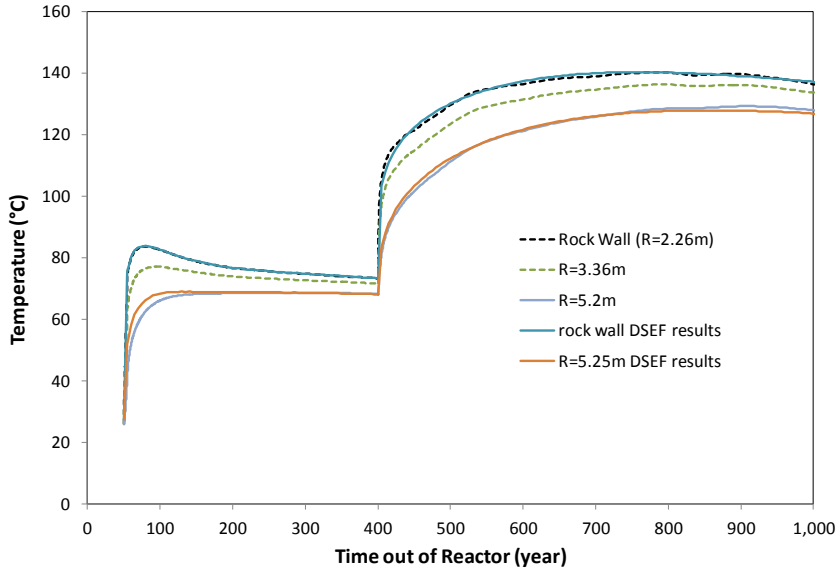

Figure 6. Temperature evolution at several compliance points for the 350-year ventilation scenario.

Due to the longer ventilation period, we expect the stronger impact on the saturation profiles shown in Figure 7. We can see accordingly that the desaturation of the near-field rock is stronger (higher gas saturations) and that it extends further into the host rock. At the rock wall, a gas saturation value of ~0.63 is achieved prior to ceasing ventilation. Just 0.3 meters into the host rock, the gas saturation value has a maximum of ~0.41 (34% less than close to the rock wall). At a radial distance of 3.36 meters, 5.25 meters, and 11.25 meters, gas saturation values are ~0.18, 0.08, and 0.01, respectively. After ventilation

stops, we observe a slightly longer resaturation time of ~50 to 75 years, whereas (as mentioned above) it takes about 10 years to resaturate the desaturated zone for the 40-year ventilation scenario.

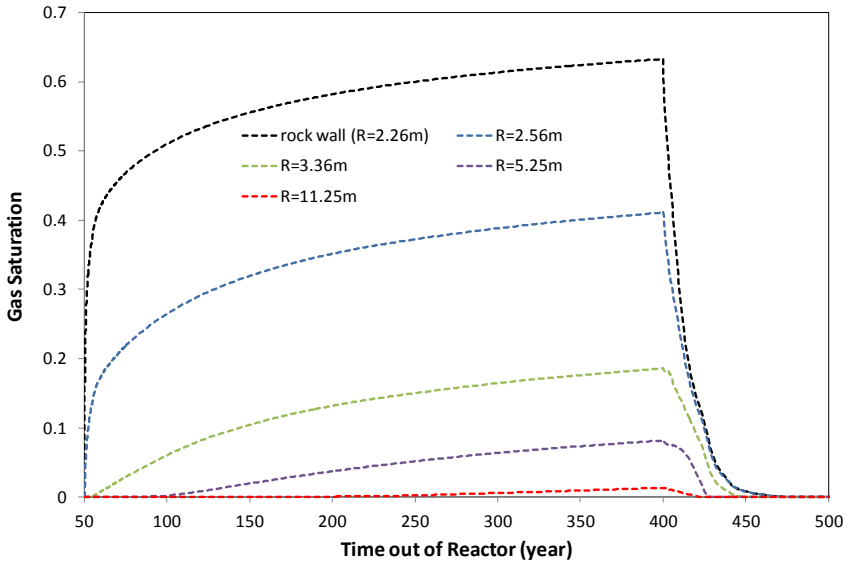

Figure 7. Gas saturation evolution at several compliance points for the 350-year ventilation scenario.

3.2.2.2 Sensitivity Analysis

The thermal conductivity and hydraulic permeability of the host rock are two of the most important properties determining the TH evolution in a clay formation. We therefore conducted a series of sensitivity analyses to illustrate how model results are affected by these parameters. We first evaluated how the water saturation-dependent thermal conductivity affects the TH changes in the host rock and then investigated the TH response of the host rock, if K_{TH} varies between its maximum/minimum published values and the permeability changes by a factor of 2 (from the base case of 5×10^{-19} m^2). Finally, the effect of a DRZ on the desaturation of host rock is evaluated.

Effect of Saturation-dependent Thermal Conductivity

The assumption that thermal conductivity remains unchanged over the course of heating and desaturation of host rock is a necessary simplification for the DSEF calculation, since moisture conditions are not solved there. However, it is known that the thermal conductivity of a porous medium decreases if the medium become drier. By allowing the thermal conductivity to change with the water saturation, we can evaluate inaccuracies introduced by assuming that the thermal conductivity remains unchanged. Typically, the effective thermal conductivity K_{TH} is a function of S_l, K_{wet} and K_{dry}. Among several empirical published functions (e.g., Tang et al., 2008), here we use Eq. (1), which is implemented in TOUGH2 to calculate the changes of K_{TH} when S_l changes. In the sensitivity run, K_{wet} is 1.75 W/m*K and a K_{dry} of 1.48 W/m*K is calculated according to the following equation:

$$K_{dry} = \alpha\left(\frac{V_{air}}{V}\right) + K_{wet} \qquad (2)$$

where $\alpha = -K_{wet}$ and $\left(\frac{V_{air}}{V}\right)$ = 0.15 (porosity). To understand the effect of saturation-dependent thermal conductivity on the TH evolution in host rock, we compare the temperature at several locations calculated in the sensitivity run (K_{Wet} = 1.75 W/m K and K_{Dry} = 1.48 W/m K) and base case (K_{Wet} = K_{Dry} = 1.75 W/m K). Very minimal differences are observed, as exemplified with the temperature evolution for the 350-year ventilation scenario (Figure 8). This is due to the fact that in the sensitivity run, K_{TH} only exhibits very small variation within the small desaturated zone — the lowest value can only go down to 1.68 in the 40-year ventilation scenario and to 1.64 in the 350-year ventilation scenario. Current model results show that the assumption that thermal conductivity remains unchanged over the course of heating and desaturation of a host rock does not introduce a noticeable miscalculation of the thermal evolution. It is noteworthy, however, that the K_{dry} used in the sensitivity run is taken from an empirical equations, and it is fairly close to the K_{wet}. In a case in which K_{dry} is much lower than K_{wet} , the conclusion might be different.

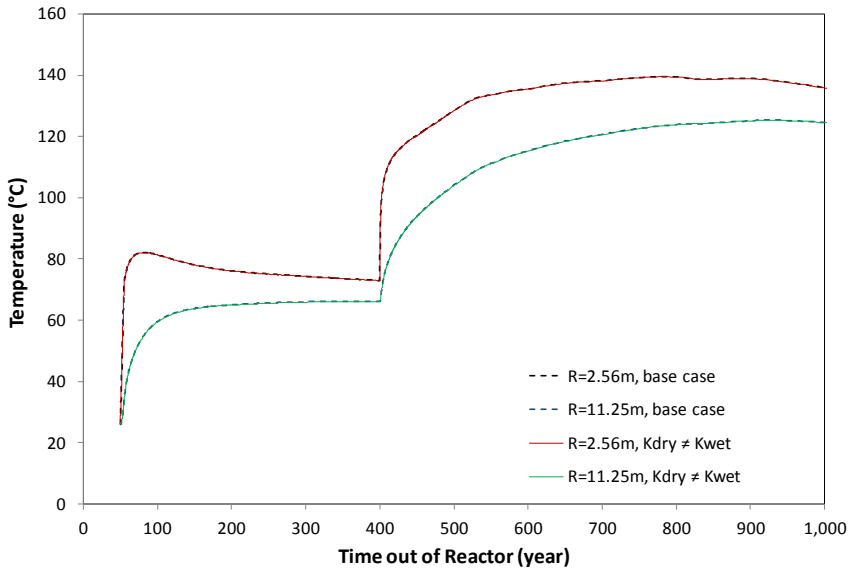

Figure 8. Temperature evolution for the 350-year ventilation scenario: sensitivity run (K_{Wet} = 1.75 W/m K and K_{Dry} = 1.48 W/m K) versus base case (K_{Wet} = K_{Dry} = 1.75 W/m K).

Sensitivity to K_{TH} Variation

In this case we tested the sensitivity of temperature and water saturation to thermal conductivity, as typically there are some uncertainties in measured thermal conductivity. For example, according to Bossart (2011), Opalinus Clay, has a K_{TH} range from 1.00 W/m*K to 3.00 W/m*K. Sensitivity runs with maximum/minimum published values were conducted and results are discussed below.

In one of the sensitivity runs, we use a K_{TH} of 1.00 W/m*K by setting $K_{wet} = K_{dry} = 1.00\ W/m\ K$. In Figure 9, for the 40-year ventilation scenario, the rock wall temperature is ~50°C higher in the sensitivity run than in the base case. Figure 10 illustrates the changes in gas saturation; in the sensitivity run, the gas saturation value is ~0.01 higher than that in the base case. This corresponds to a 2% increase in gas saturation. Similarly in Figure 11 for the 350-year ventilation scenario, a difference of 34°C exists at the rock wall between the sensitivity run and the base case. For gas saturation profiles in the 350-year ventilation scenario, Figure 12 shows a 1.5% increase in gas saturation at the rock wall.

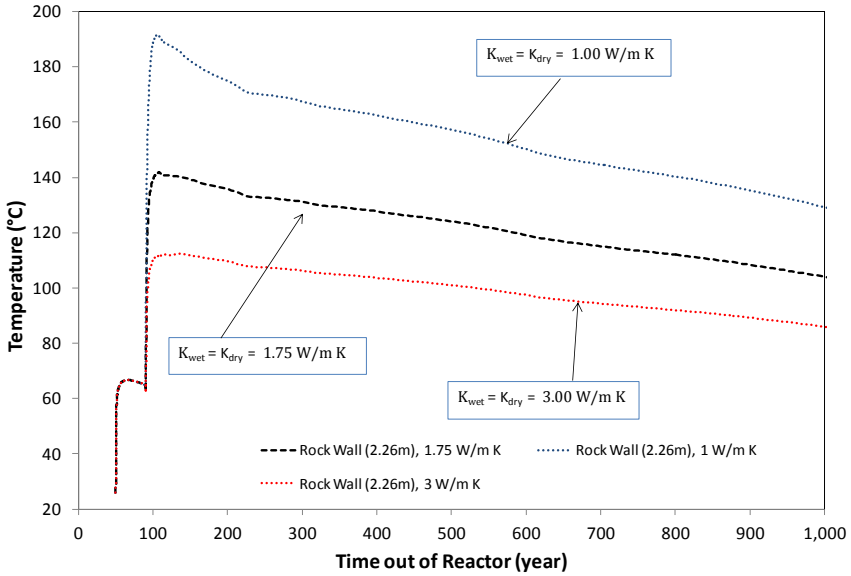

Figure 9. Temperature evolution at the rock wall for the 40-year ventilation scenario: Sensitivity run to the K_{TH}.

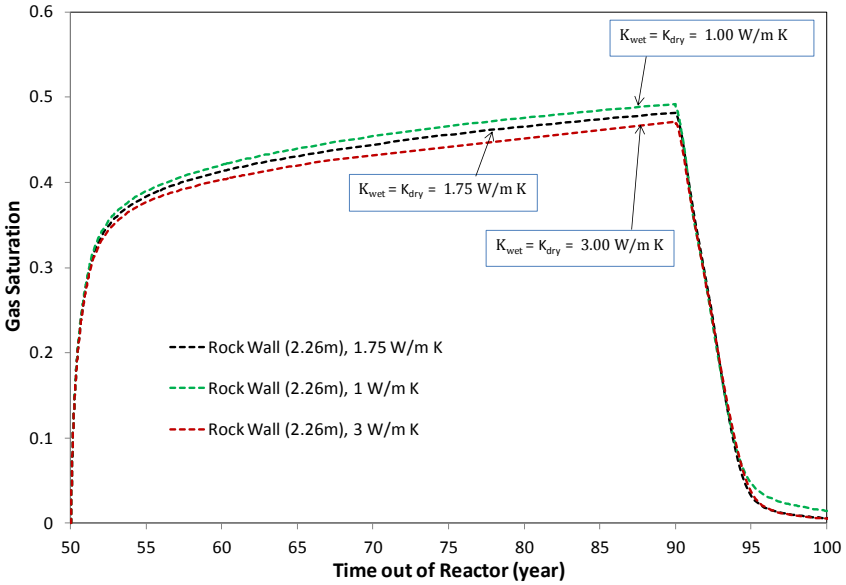

Figure 10. Gas saturation evolution at the rock wall for the 40-year ventilation scenario: Sensitivity run to the K_{TH}.

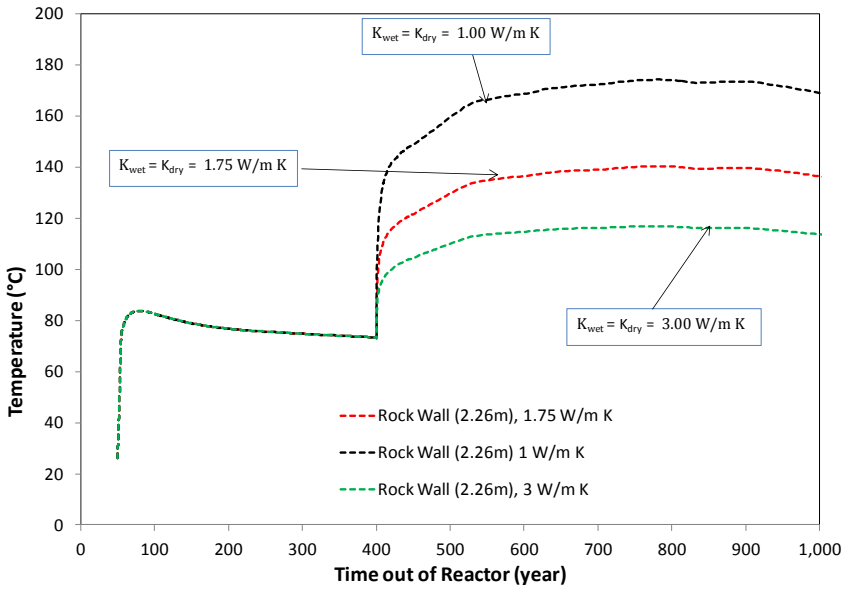

Figure 11. Temperature evolution at the rock wall for the 350-year ventilation scenario: Sensitivity run to the K_{TH}.

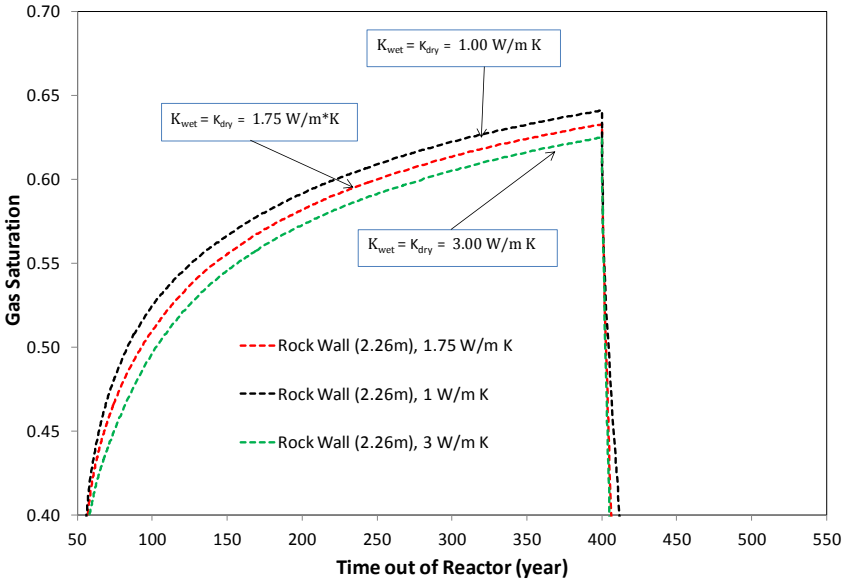

Figure 12. Gas saturation evolution at the rock wall for the 350-year ventilation scenario: Sensitivity run to the K_{TH}.

In another sensitivity run, we used the K_{TH} of 3.00 W/m K by setting $K_{wet} = K_{dry} = 3.00\, W/m\, K$. Increasing K_{TH} results in faster heat dissipation and therefore the temperature at the rock wall in the clay formation is expected to be lower. In Figure 9, a decrease of 33°C is achieved at the rock wall for the 40-year ventilation scenario when increasing K_{TH} to 3.00W/m K. For gas saturation, Figure 10 shows a 2% decrease in gas saturation at the rock wall compared to the base case. For the 350-year ventilation scenario, a decrease of 23°C in temperature is observed at the rock wall and a decrease of 1% in gas saturation is achieved at the rock wall in the sensitivity run.

A lower K_{TH} value leads to higher temperature in the clay formation, which subsequently results in a slightly larger desaturated zone. For instance, in the 40-year ventilation case, the desaturated zone extends 3.63 meters into the host rock when K_{TH} is 1.00W/m*K in the sensitivity run compared to 3.26 meters when K_{TH} = 1.75 W/m*K in the base case. Similarly, increasing K_{TH} lowers the desaturated zone, but the effect of K_{TH} on the range of desaturated zone is fairly minor.

Sensitivity to Permeability

Permeability affects the migration of fluids and gases in a porous medium, and is a function of porosity, which in turn depends on grain shape, size, and sorting. In our sensitivity run, we increased the permeability by a factor of 2 to illustrate how a change in permeability affects the TH behavior in the host rock. Increasing permeability leads to a larger desaturation zone (see Figures 13 and 14), due to faster moisture migration during ventilation. Note that in Figure 14, it is the thickness in the direction vertically above the drift and de-saturation reaches the left and right boundary. Although in both the base and sensitivity cases, the thermal conductivity is not a function of liquid saturation (which does not allow us to evaluate the effect of increasing permeability on saturation and subsequently on the temperature), we would expect that permeability has little effect on temperature because (as demonstrated in the first part of Section 3.3.2.2) liquid saturation changes affect temperature insignificantly.

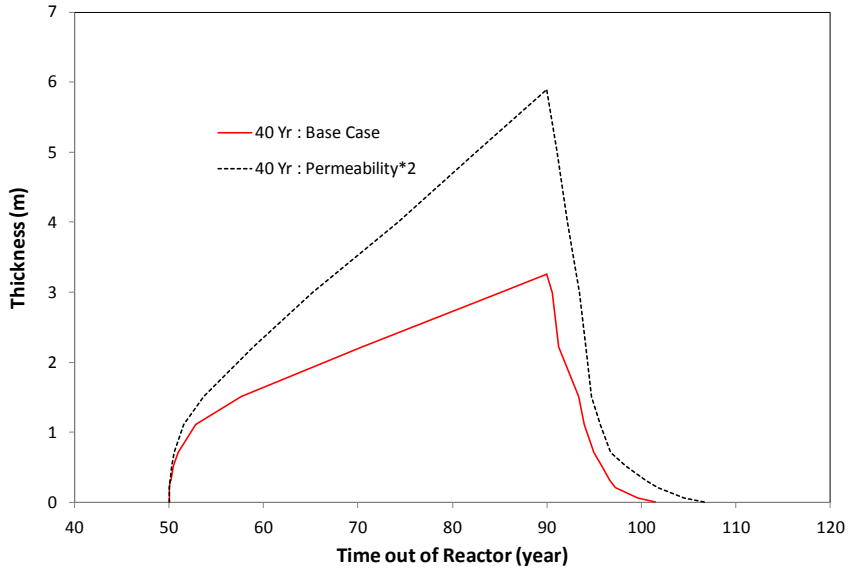

Figure 13. Thickness of desaturated zone for the 40-year ventilation scenario: base case and sensitivity run with doubled permeability.

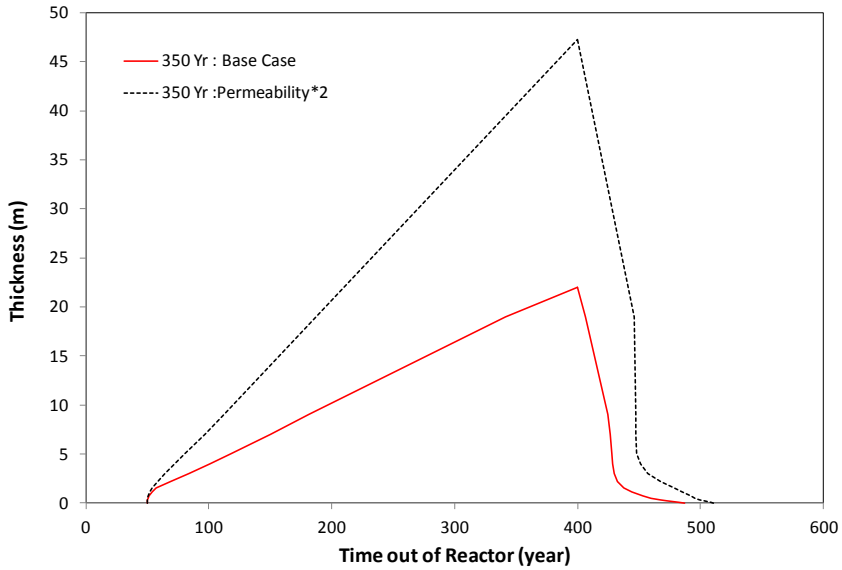

Figure 14. Thickness of de-saturated zone for the 350-year ventilation scenario: base case and sensitivity run with doubled permeability.

The effect of a DRZ

A DRZ (Disturbed Rock Zone) has significant implications for the overall performance of a disposal system. The thickness and permeability of a DRZ can vary a great deal. For example, DRZ for Opalinus Clay (Thury, 2002) ranges from 0.5 to 3 m thick and has a permeability of one to several orders of magnitude higher than undisturbed rock. The base model does not consider a DRZ in the host rock, in order to be consistent with the DSEF calculation. In a sensitivity run, we increase the permeability by one order of magnitude for the 1 m thick host rock in the vicinity of the rock wall, to mimic the effect of a DRZ on the desaturation of the host rock. Figures 15 and 16 show the gas saturation at several points for the 40-year ventilation and 350-year ventilation scenarios, respectively. The existence of a DRZ leads to lower gas saturation at rock wall but higher gas saturation inside the host rock, which essentially shows a flatter gas saturation gradient from rock wall toward inside area. Because of the higher permeability of a DRZ, water moves out faster, and therefore the de-saturated zone penetrates deeper into the host rock.

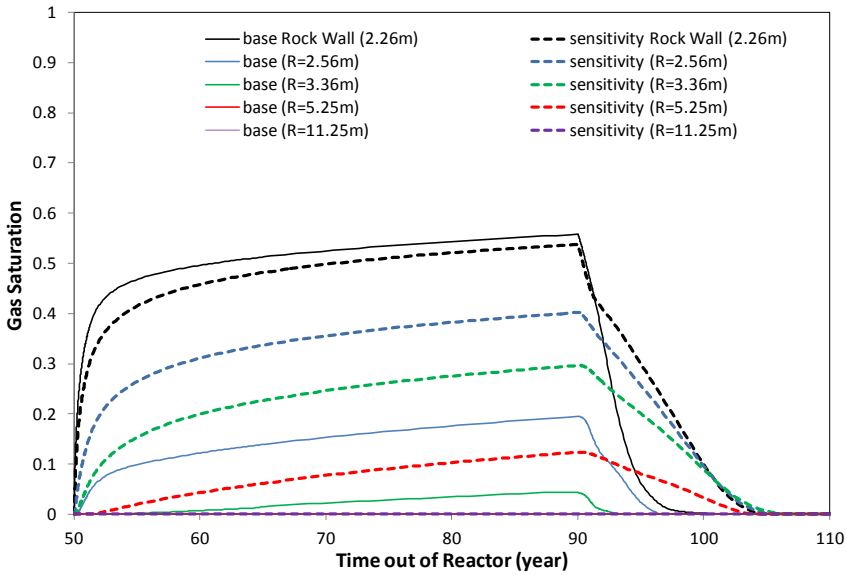

Figure 15. Gas saturation evolution at several points for the 40-year ventilation scenario: Sensitivity run with DRZ and base run without DRZ.

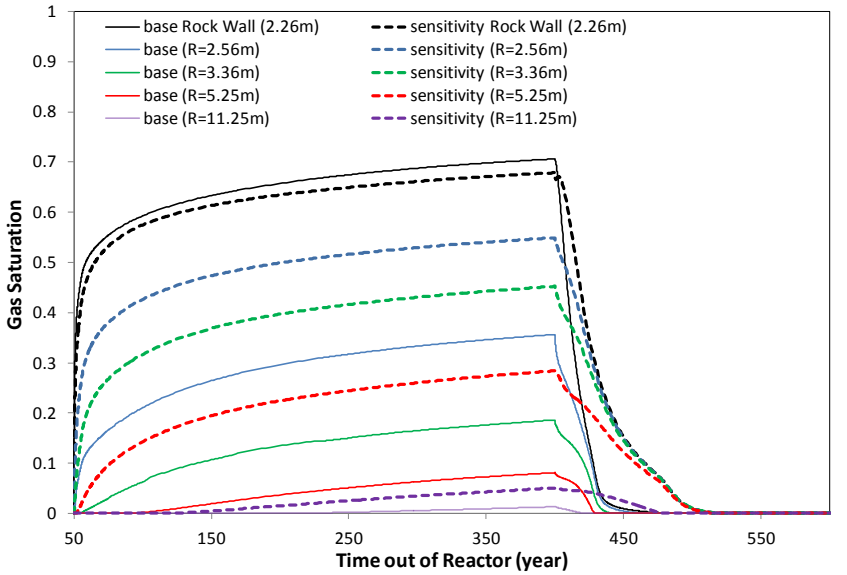

Figure 16. Gas saturation evolution at several points for the 350-year ventilation scenario: Sensitivity run with DRZ and base run without DRZ.

4. THM model based on more realistic geometry

4.1 Modeling scenario

The model presented in Section 3 assumes an axi-symmetrical layout of canister backfill in the drift. This is a necessary assumption for DSEF, as it greatly simplifies the calculation of the thermal evolution in the host rock. However, as shown in Figure 17, the waste package will be emplaced on the floor of the drift,

undergoes ventilation, and later will be surrounded by bentonite backfill. At the bottom, the water package will directly contact with the concrete liner, whereas on the top of the drift, bentonite backfill separates the canister and concrete liner. As a result, the heat transport from canister to the top and bottom is different, and the thermal evolution at the top of the rock will be different from that at the bottom. In this section, we present a THM model based on the geometry shown in Figure 17. Here again, we model a drift located 500 m deep underground as shown in Figure 3, with a drift spacing of 45 m, and a waste package spacing of 20 m along the drifts. The mesh for the area surrounding the canister is shown in Figure 18.

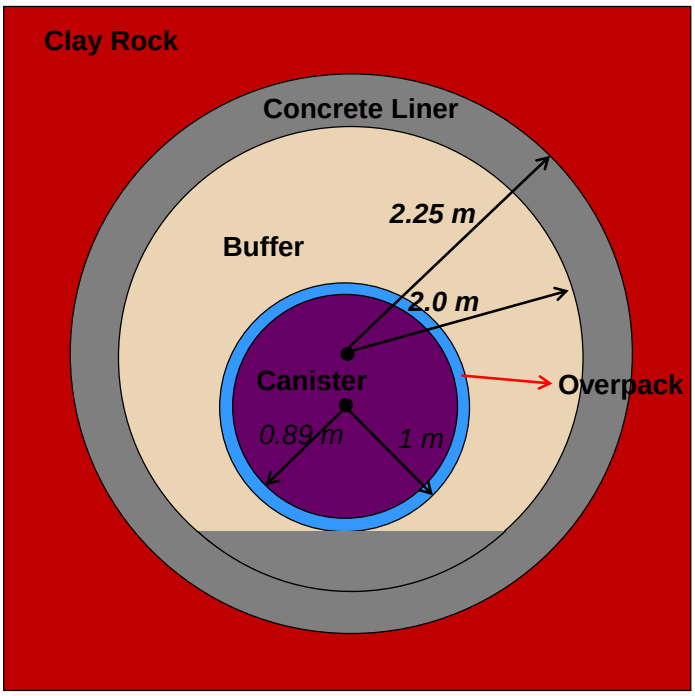

Figure 17. Geometry of a cross section of a drift for the disposal of DPC.

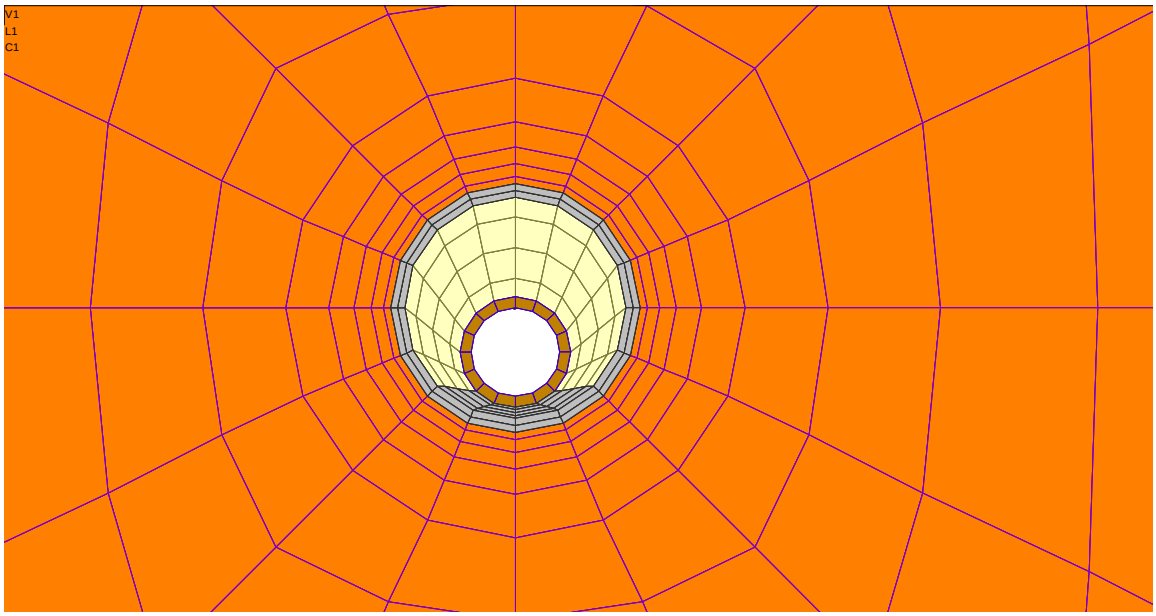

Figure 18. Mesh used in THM model for the DPC disposal shown in Figure 17.

In this section, we modeled only the 40-year ventilation scenario; the 350-year ventilation scenario is helpful for understanding the effect of prolonged ventilation, but it is fairly challenging to maintain active ventilation for 350 years. We therefore did not consider the 350-year ventilation scenario here. During the ventilation period, the temperature at the canister surface calculated by DSEF is used as the boundary condition, i.e., the temperature at the canister is fixed. The relative humidity of the air in the drift tunnel is about 53%. After ventilation ends, a heat source term is used to represent the canister, and the heat release rates are shown in Figure 19, which are calculated by dividing the heat release of a waste package (32 PWR and 40 GWd/MTHM) by the waste package spacing, 20 m.

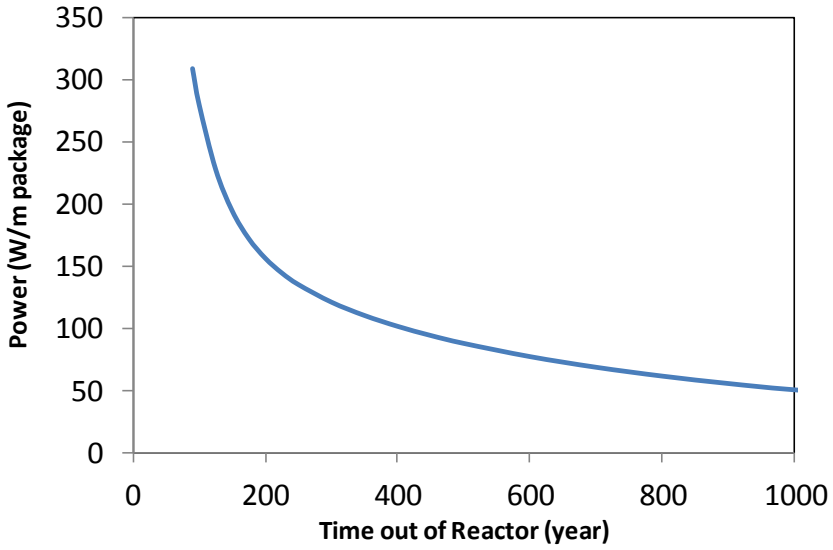

Figure 19. Heat load for the 2D THM model

4.2 The mechanical models and properties

A linear elastic swelling model (Rutqvist et al., 2011) is used for bentonite backfill. Under mechanically constrained conditions, a swelling stress, σ_s, is linearly proportional to the saturation:

$$d\sigma_s = 3K\beta_{sw}ds_l \tag{3}$$

where K is the bulk modulus and β_{sw} is a moisture swelling coefficient. In this report, β_{sw} is 0.0108.

Table 2. Thermal, mechanical and hydrodynamic parameters for concrete liner

Parameter	Concrete liner
Grain density [kg/m^3]	2700
Porosity ϕ	0.15
Saturated permeability [m^2]	$5.0\cdot10^{-20}$
Relative permeability, k_{rl}	$K_{rl} = S^3$
Van Genuchten α [1/Pa]	$3.3\cdot10^{-8}$
Van Genuchten m	0.3
Compressibility, β [1/Pa]	$5.0\cdot10^{-8}$
Thermal expansion coeff., [1/K]	$1.0\cdot10^{-4}$
Dry specific heat, [J/kg^{o}C]	1000
Thermal conductivity [W/m K]	1.35(dry)/1.6(wet)*
Tortuosity for vapor phase	$\phi^{1/3}S_g^{10/3}$
Young's modulus, (GPa)	23
Poisson's ratio	0.2

An elastic model was used for the concrete liner and argillite. The rock properties for argillite are listed in Table 1; they correspond to that of Opalinus Clay, with values taken from Gens et al. (2007) as well as Corkum and Martin (2007). Here, we utilize the FLAC3D ubiquitous joint model, a model also used by Corkum and Martin (2007) when simulating previous *in situ* experiments in Opalinus Clay at Mont Terri. The theory and implementation of this model in FLAC3D is described in the FLAC3D manual (Itasca, 2009). The rock properties for concrete liner are listed in Table 2, which are mostly taken from Kim et al. (2013) except for thermal conductivity. Gibbon and Ballim (1998) measured the thermal conductivity of concrete and reported values from 0.75 to 1.2 W/m K, which fall into 0.6–2.6 range of other publications they cited. Here, we took the median value 1.6 for wet conditions, and the thermal conductivity for dry concrete is calculated by Equation (2), which yields 1.35.

4.3 Model results

Temperature evolution exhibits a great deal of asymmetry in the area surrounding the waste package (canister), as shown in Figure 20. Because the concrete and host rock have higher thermal conductivity than bentonite backfill, and the canister is laid directly upon the concrete liner, the heat dissipates faster at the bottom of canister, where the temperature is thus lower than that at the top of canister, where backfill separates the canister and concrete liner. Then, from the inner surface of the liner to the outer surface of the liner and into the rock, those located at the bottom have higher temperatures. In the concrete liner, peak temperature at the bottom is typically 7–10°C higher than that at the top, and the temperature in the liner at the bottom also peaks earlier. At the rock wall, at the bottom of the drift, the maximum temperature is about 126°C whereas at the top it is about 120°C. In terms of peak temperature at the rock

wall, the TOUGH model results are lower than that obtained through DSEF. Typically area close the central line of canister is hotter and area between canisters is cooler, but the TOUGH2 model, because it is a 2-D cross section, shows actually the average temperature conditions. On the contrary the DSEF shows the localized high temperature at the central line of the canister. Also shown in Figure 20 are the temperature evolution inside the host rock at 1.4 m and 10 m away from the rock wall. Even 10 m away from the rock wall, at the top and bottom of the drift, the temperature still differs by 2°C. Figure 21 shows the temperature in the backfill starting from 90 years when the backfill is emplaced. The maximum temperature reaches about 140°C and remains around 120°C after 1000 years.

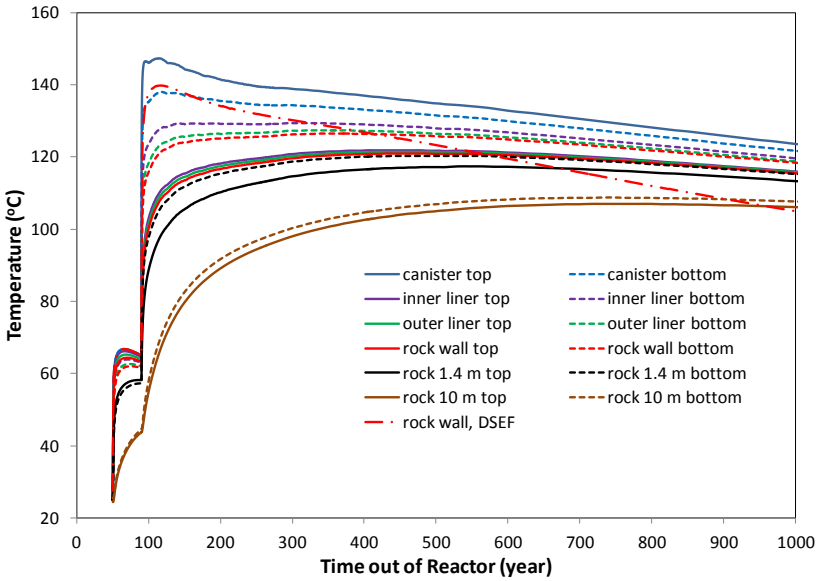

Figure 20. Temperature evolution at several locations, solid lines represent the temperature at locations above of the waste package and dashed lines are the temperature at locations below the waste package.

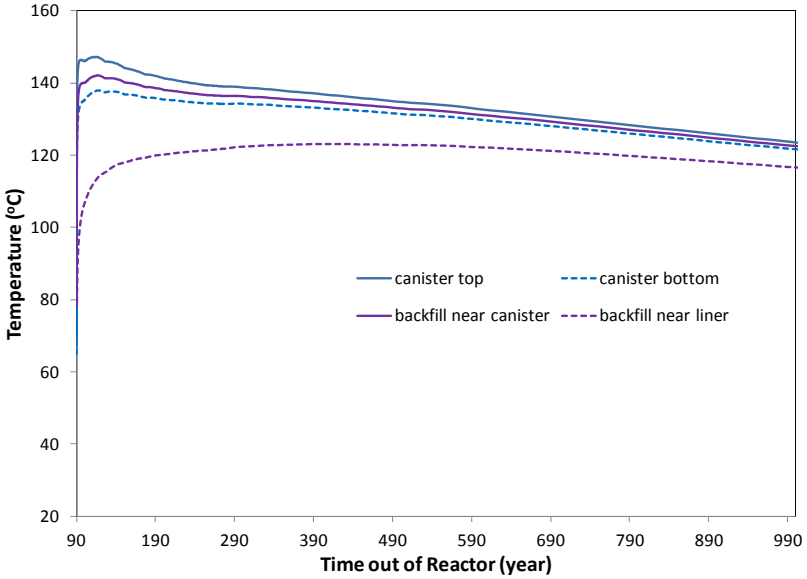

Figure 21. Temperature evolution at canister surface and in the backfill

Figure 22 shows the gas saturation at different locations. During the ventilation period, at the top of the drift, the liner and host rock undergo stronger desaturation than at the bottom of the drift. After the emplacement of backfill, concrete liner and host rock are quickly hydrated from the far field, and gas saturation decreases sharply. However, the concrete liner and host rock remain unsaturated until 280 years, although the gas saturation is fairly low.

Initially, the backfill has a gas saturation of 0.35, but after being emplaced in the hot drift, evaporation drives the backfill to even drier conditions within a short period (Figure 23). After that, backfill is hydrated from the surrounding environment, and gas saturation decreases quickly. But, as with the concrete liner, the backfill will not reach full saturation until 280 years.

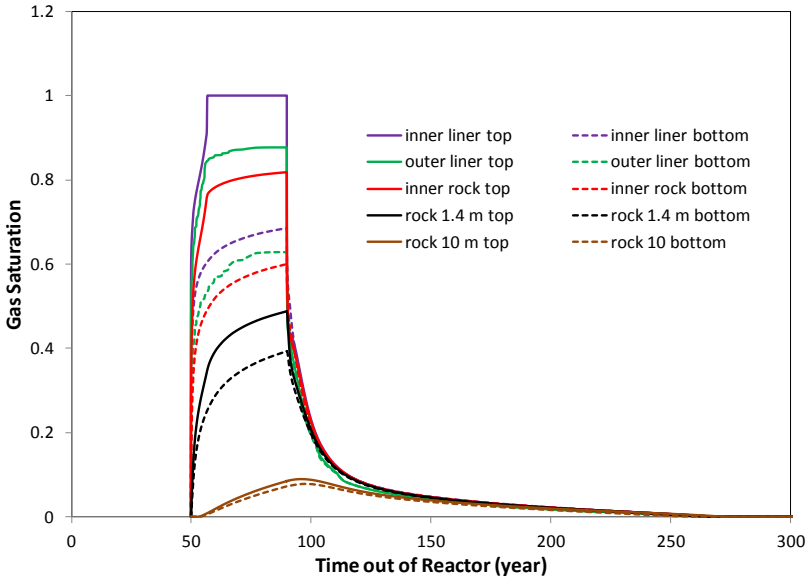

Figure 22. Gas saturation evolution at several locations. Solid lines represent the temperature at locations above the waste package, and dashed lines indicate the temperature at locations below the waste package.

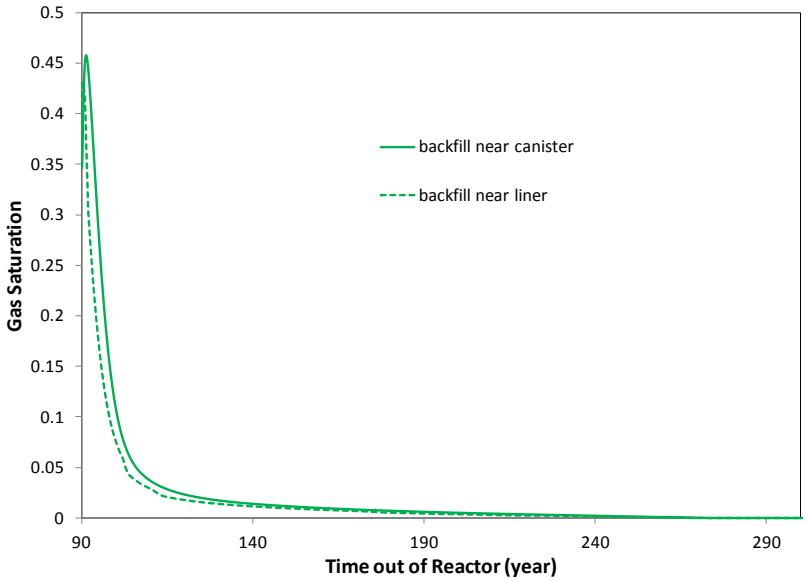

Figure 23. Gas saturation evolution at two points in the backfill.

The whole system undergoes dramatic changes in pore pressure. Starting from hydrostatic conditions, the ventilation quickly drives the pore pressure in the concrete and host rock to atmospheric pressure as in the open drift. Even after the cessation of ventilation and emplacement of backfill, the pore pressure remains low as the media remains unsaturated. After it becomes fully saturated everywhere, the pore pressure quickly goes up, and thermal pressurization makes the pressure even higher than hydrostatic fluid pressure, which is 4.5×10^6 Pa under ambient temperature conditions.

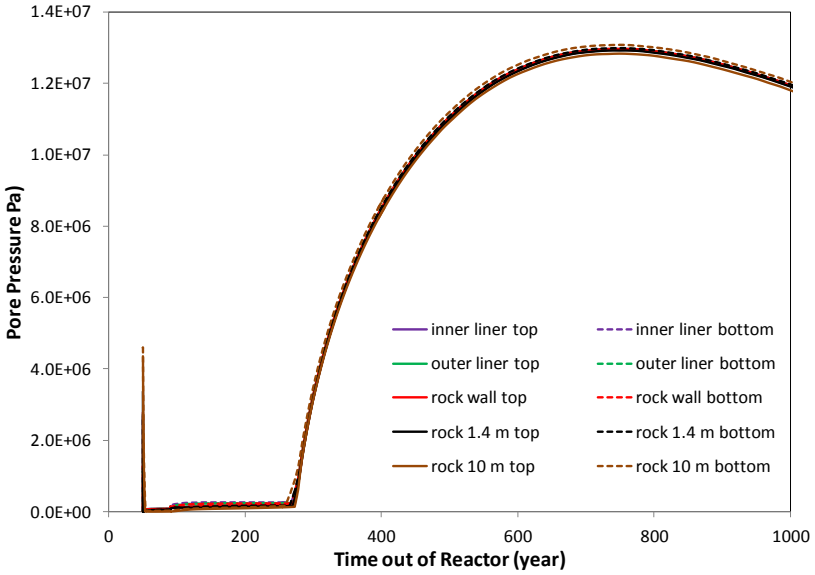

Figure 24. Pore pressure evolution at several locations. Solid lines represent the pressure at locations above the waste package, and dashed lines indicate the pressure at locations below the waste package.

Figure 25 presents the evolution of total stresses within the backfill near the canister. The negative values indicate compressive stress. The evolution of the total stress results mainly from the poro-elastic stress caused by changes in fluid pressure whereas the effects of moisture swelling (saturation change) and temperature are relatively small in this case. In comparison with the stress evolution in backfill for smaller canisters (4 PWR canister) as assumed in the model of Rutqvist et al. (2014), the stress is higher, mainly because of higher pore pressure resulting from thermal pressurization. The stress changes within the backfill are fairly uniform.

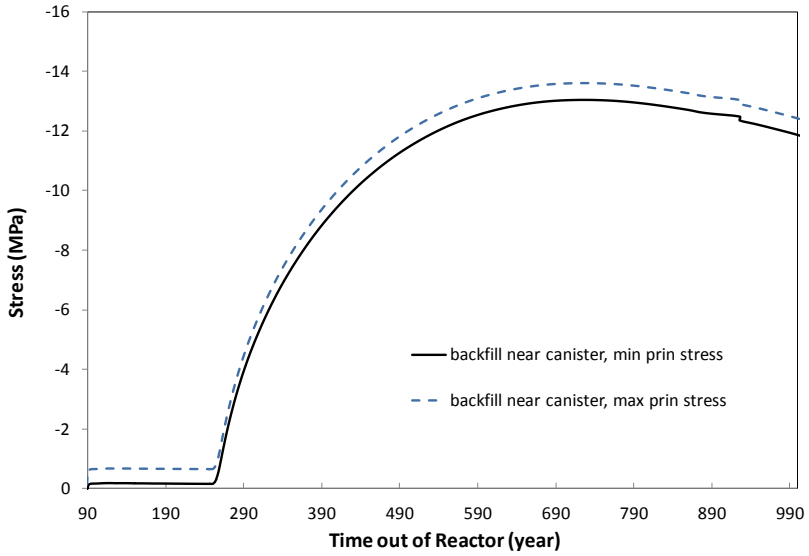

Figure 25. Minimum and maximum compressive principal stress within the backfill near the canister.

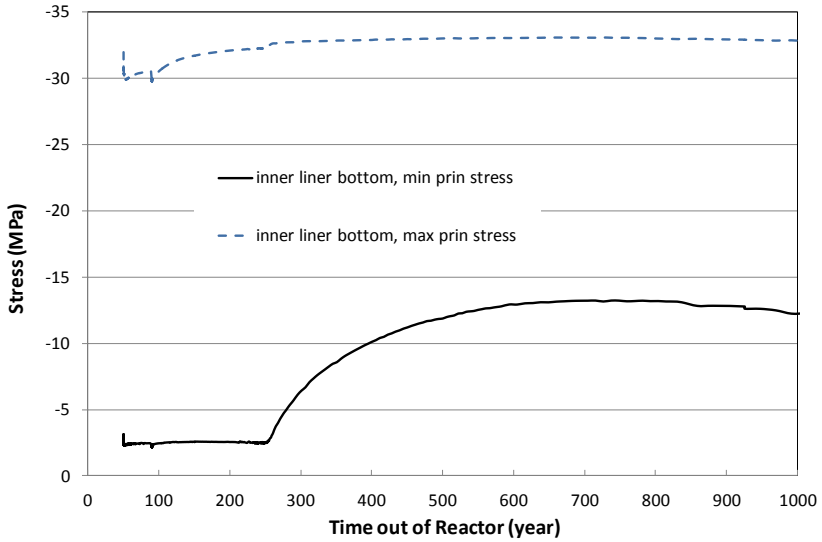

Figure 26. Minimum and maximum compressive principal stress within the concrete liner at the bottom.

Figure 26 shows the maximum and minimum compressive principal stress in the liner at the bottom of the drift. Increases in pore pressure lead to significant increases in minimal compressive principal stress in the liner, and then a gradual decrease as the pore pressure decreases. The maximal compressive principal stress, which is largely along the horizontal direction, still keeps increasing at 1000 years.

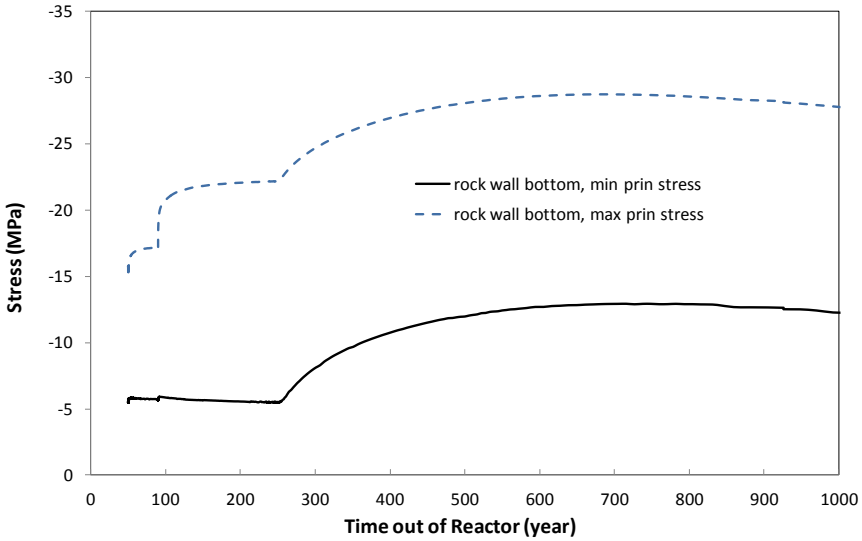

Figure 27. Minimum and maximum compressive principal stress at the rock wall.

Figure 27 shows the maximum and minimum compressive principal stress at the rock wall. Results show a significant increase in the maximum compressible principal stress, which is affected by both the local temperature change and fluid pressure changes. The minimum principal stress, which is the stress normal to the drift wall at this location, increases along the increasing stress within the buffer.

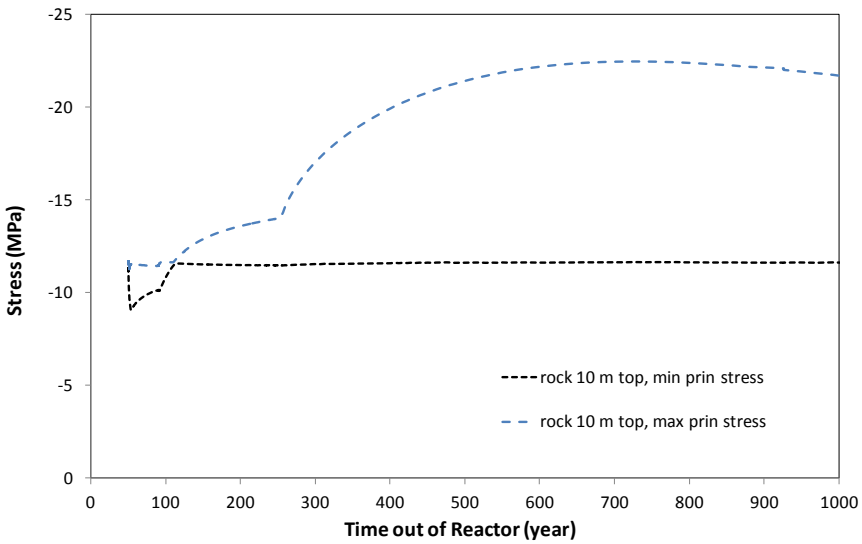

Figure 28. Minimum and maximum principal stress within the host rock 10 m away from the rock wall.

Figure 28 shows the maximum and minimum principal stress with the host rock 10 m away from the rock wall. While the minimum principal stress does change much after the initial perturbation by desaturation and resaturation, there is a significant increase in the maximum principal stress, which is affected by the no-displacement lateral boundary conditions.

5. CONCLUSIONS AND FUTURE WORK

5.1 Conclusion

Recently the technical feasibility of direct disposal of DPCs has been analyzed in UFDC (Hardin and Voegele, 2013; Hardin et al., 2013). Preliminary analysis has indicated that direct disposal of DPC could be technically feasible, at least for certain disposal concepts (Hardin et al., 2013). The disposal of DPC in argillaceous sedimentary rock is one of the concepts that has been proposed. Because of the large inventory and (therefore) higher heat-release rate of the DPC, the temperature limit in an argillite repository must be raised above 100°C to avoid a large repository footprint or long-term surface storage. Important issues must be addressed for better assessment of the performance implications of substantially higher temperature. One of the issues is thermal (T), hydrological (H), mechanical (M) chemical (C) alterations in the EBS and host rock.

Significant knowledge has been gained in the UFDC and international research work related to the disposal of small canisters in argillaceous host rock—knowledge which can applied to the disposal of DPC, to some extent. However, in terms of using 2D and 3D models to predict the changes in EBS and argillaceous host rock, disposal of DPC has some special features that differ from the disposal of small canisters, which make previous models developed for small canisters inapplicable. These features include an initial ventilation period, larger drift, and asymmetric layout of waste package and EBS, and possibly a thicker concrete liner or steel liner to maintain stability. Therefore, disposal of DPCs in argillaceous host rock needs its own series of 2D and 3D models to evaluate THMC processes in the EBS and host rock. In this report, we document initial progress toward building 2D and 3D models for evaluating THMC processes in the EBS and argillaceous host rock for disposal of DPCs. This report documents two major accomplishments to date in FY14.

First, a 2-D TH model using TOUGH2 (Pruess et al., 1999) was conducted to evaluate the desaturation of argillaceous host rock as a result of heating, based on the temperature calculated by Disposal Systems Evaluation Framework (DSEF). The temperature at the rock wall obtained by DSEF is used as a boundary condition. A comparison between TOUGH2 and DSEF models of temperature within the host rock shows very similar results, which indicates that changes in thermal conductivity with water saturation have minimal effect on the temperature profile. The comparison therefore confirms that assuming constant thermal conductivity in DSEF might not have a significant impact on the calculated temperature. Model results also show that ventilation leads to a desaturated zone in the host rock, ranging from a couple of meters to tens of meters. Longer ventilation, higher permeability, and the existence of a DRZ enlarges the thickness of the desaturated zone.

Second, we developed a 2-D THM model for a more realistic layout geometry of waste package and backfill to examine the THM behavior in backfill and host rock. In order to be aligned with DSEF, the model mentioned above assumes an axi-symmetrical layout of canisters, and backfill in the drift. However, a more realistic condition is that a waste package will be emplaced on the ground of drift, and its bottom will be in direct contact with a concrete liner, whereas at the top of the drift, bentonite backfill separates the waste package and concrete liner. Several observations can be made from model results:

1. Moderate temperature disparity in the backfill and liner at the top and bottom of drift has been observed, ranging from 7°C to 10°C. But such a disparity diminishes for areas further inside the host rock.
2. During ventilation, the concrete liner and host rock at the top of drift undergo more desaturation than that at the bottom. After the emplacement of backfill, resaturation takes place, but it takes about 200 years to reach full saturation.

3. Significant increases in stresses have been observed, due to increases in pore pressure and thermal stress.

5.2 Future work

For the remaining months in FY14 and subsequent years, the following work will be conducted:

1. Studying the chemical changes in the concrete liner and host rock with a THC model. Preliminary analyses of the feasibility of direct disposal of DPC conclude that a 50–100 year ventilation period is needed to keep the temperature at a manageable level. During ventilation, the dryout in the concrete liner and host rock induced significant mineral changes, which should be studied in the near future.
2. Developing a 3-D model to study the THMC alteration in the disposal system for DPC. One lesson learned from current modeling exercise is that a 3-D model is needed to accurately calculate the maximum temperature in the disposal system, since when and where the maximum temperatures might appear cannot be accurately simulated by a 2-D model. Typically, the temperature is higher along the central line of waste package and is lower in the area between two waste packages. A 2-D model can only provide average conditions in the vicinity of the waste package.

6. ACKNOWLEDGMENT

Funding for this work was provided by the Used Fuel Disposition Campaign, Office of Nuclear Energy, of the U.S. Department of Energy under Contract Number DE-AC02-05CH11231 with Lawrence Berkeley National Laboratory.

7. REFERENCES

Bossart, P., (2011). Characteristics of the Opalinus Clay at Mont Terri, http,//www.mont-terri.ch/internet/mont-terri/en/home/geology/key_characteristics.html

Corkum A.G., Martin C.D., (2007). The mechanical behaviour of weak mudstone (Opalinus Clay) at low stresses. Int. J. Rock Mech. Min. Sci. 44: 196-209.

De Windt, L., Palut, J.M., (1999). Tracer feasibility experiment FM-C, DI. In: Thury, M., Bossart, P. Eds., Mont Terri Rock Laboratory: Results of the Hydrogeological, Geochemical and Geotechnical Experiments Performed in 1996 and 1997. Geol. Ber., vol. 23. Swiss National Hydrological and Geological Survey, Bern.

Gens, A., Garitte, B., Wileveau, Y., (2007). In situ behaviour of a stiff layered clay subject to thermal loading: Observations and interpretation. Geotechnique. 57: 207-228.

Gibbon, G.J., Ballim, Y. (1998). Determination of the thermal conductivity of concrete during the early stages of hydration. Magazine of Concrete Research 50, 229-235

Greenberg, H.R., Sharma, M., Sutton, M., Barnwell, A.V., (2012). *Repository Near-Field Thermal Modeling Update Including Analysis of Open Mode Design Concepts*. Lawrence Livermore National Laboratory. LLNL-TR-572252

Hardin E., Voegele, M., (2013). Alternative Concepts for Direct Disposal of Dual-Purpose Canisters, FCRD-UFD-2013-000102 Rev. 0, Sandia National Laboratories, February 2013

Hardin, E., Clayton, D., Howard, R., Scaglione, J.M., Pierce, E., Banerjee, K., Voegele, M.D., Greenberg, H., Wen, J., Buscheck, T.A., Carter, J.T., Severynse, T., Nutt, W.M., (2013). Preliminary Report on Dual-Purpose Canister Disposal Alternatives (FY13), August, 2013, FCRD-UFD-2013-000171 Rev. 0

Harrington, J.F., Horseman, S.T., (1999). Laboratory experiments on hydraulic and osmotic flow. In: Thury, M., Ž. Bossart, P. Eds. Mont Terri Rock Laboratory: Results of the Hydrogeological, Geochemical and Geotechnical Experiments Performed in 1996 and 1997. Geol. Ber., vol. 23. Swiss National Hydrological and Geological Survey, Bern.

Hicks, T.W., White, M.J., Hooker, P.J., (2009). Role of Bentonite in Determination of thermal Limits on Geological Disposal Facility Design. Galson Sciences Limited

Itasca (2009). FLAC3D V4.0, Fast Lagrangian Analysis of Continua in 3 Dimensions, User's Guide. Itasca Consulting Group, Minneapolis, Minnesota.

Kim, H.-M., Rutqvist, J., Jeong, J.-H., Choi, B.-H., Ryu, D.-W, Song, W.-K., (2013). *Characterizing Excavation Damaged Zone and Stability of Pressurized Lined Rock Caverns for Underground Compressed Air Energy Storage*. Rock Mechanics and Rock Engineering 46(5): 1113-1124.

NAGRA (1989). Sedimentstudie-Zwischenbericht, 1988. Moglichkeiten zur Endlagerung Langlebiger Radioaktiver Abfalle in den Sedimenten der Schweiz. NAGRA Technischer Bericht 88-25, NAGRA, Baden, Switzerland. Also executive summary in English, NAGRA Technical Report 88-25E.

Pruess, K., Oldenburg, C., Moridis, G., (1999). *TOUGH2 User's Guide, Version 2.0*, Lawrence Berkeley National Laboratory, Berkeley, CA.

Rutqvist, J., Ijiri, Y., Yamamoto, H., (2011). Implementation of the Barcelona Basic Model into TOUGH-FLAC for simulations of the geomechanical behavior of unsaturated soils. Computers & Geosciences, 37, 751–762.

Rutqvist, J., Zheng, L., Chen, F., Liu, H.-H., Birkholzer, J.T., (2014). Modeling of Coupled Thermo-Hydro-Mechanical Processes with Links to Geochemistry Associated with Bentonite-Backfilled Repository Tunnels in Clay Formations. Rock Mechanics and Rock Engineering 47(1): 167-186.

Sonnenthal, E. Chapter 5 in, Birkholzer, J., Rutqvist, J., Sonnenthal, E., Barr, D., (2008). Long-Term Permeability/Porosity Changes in the EDZ and Near Field due to THM and THC Processes in Volcanic and Crystalline-Bentonite Systems, DECOVALEX-THMC Project Task D Final Report.

Soler, J.M., (2001). The effect of coupled transport phenomena in the Opalinus Clay and implications for radionuclide transport. Journal of Contaminant Hydrology 53(1–2), 63-84.

Tang, A.M., Cui, Y., J. Le., T.T., (2008). *A Study on the Thermal Conductivity of Compacted Bentonites*. Applied Clay Science 41 181-189. 77455 Marne La Vallée CEDEX 2, France.

Thury, M., (2002). The characteristics of the Opalinus Clay investigated in the Mont Terri underground rock laboratory in Switzerland. Comptes Rendus Physique 3(7-8), 923-933.

Zheng, L., Li, L., Rutqvist, J., Liu, H-H., Birkholzer, J.T., (2012). *Modeling Radionuclide Transport in Clays*. Lawrence Berkeley National Laboratory. FCRD-UFD-2012-000128.